A dual role for mycobacterial RecO in RecA-dependent homologous recombination and RecA-independent single-strand annealing

Richa Gupta[1,2], Mikhail Ryzhikov[3], Olga Koroleva[3], Mihaela Unciuleac[4], Stewart Shuman[4], Sergey Korolev[3,*] and Michael S. Glickman[1,2,*]

[1]Division of Infectious Diseases, Memorial Sloan Kettering Cancer Center, 1275 York Avenue, New York, NY 10065, USA, [2]Immunology Program, Memorial Sloan Kettering Cancer Center, 1275 York Avenue, New York, NY 10065, USA, [3]Department of Biochemistry and Molecular Biology, St. Louis University School of Medicine, 1100 South Grand boulevard, St. Louis, MO 63021, USA and [4]Molecular Biology Program, Memorial Sloan Kettering Cancer Center, 1275 York Avenue, New York, NY 10065, USA

ABSTRACT

Mycobacteria have two genetically distinct pathways for the homology-directed repair of DNA double-strand breaks: homologous recombination (HR) and single-strand annealing (SSA). HR is abolished by deletion of RecA and reduced in the absence of the AdnAB helicase/nuclease. By contrast, SSA is RecA-independent and requires RecBCD. Here we examine the function of RecO in mycobacterial DNA recombination and repair. Loss of RecO elicits hypersensitivity to DNA damaging agents similar to that caused by deletion of RecA. We show that RecO participates in RecA-dependent HR in a pathway parallel to the AdnAB pathway. We also find that RecO plays a role in the RecA-independent SSA pathway. The mycobacterial RecO protein displays a zinc-dependent DNA binding activity in vitro and accelerates the annealing of SSB-coated single-stranded DNA. These findings establish a role for RecO in two pathways of mycobacterial DNA double-strand break repair and suggest an in vivo function for the DNA annealing activity of RecO proteins, thereby underscoring their similarity to eukaryal Rad52.

INTRODUCTION

The maintenance of genome integrity is critical to all living organisms, and the systems that repair DNA damage are diverse. Double-strand breaks (DSBs) are a particularly lethal form of DNA damage that prevent chromosome replication if not repaired. In most bacteria, homologous recombination (HR) is the dominant pathway of DSB repair and is mediated by the RecA protein, which executes homology search and strand invasion of the broken ends into an intact homologous template, resulting in faithful repair. Mycobacteria elaborate two additional DSB repair pathways: non-homologous end joining (NHEJ) and single-strand annealing (SSA) (1–4). The core components of the NHEJ pathway are Ku and DNA ligase D, which cooperate to repair DNA damage in late stationary phase caused by ionizing radiation or desiccation (5,6), to seal linearized plasmids (1,7), and to rectify I-SceI-induced chromosomal DSBs (3,6). Mycobacteria lacking RecBCD cannot execute repair via the SSA pathway, whereas cells lacking the AdnAB helicase/nuclease are partially defective for HR (3). The proteins that mediate the AdnAB-independent HR pathway, which accounts for ~50% of HR events in wild type cells, are undefined.

The bacterial RecFOR machinery supports single-strand gap repair and restart of stalled replication forks (8–10). The contribution of RecFOR to the HR pathway of DSB repair in wild-type bacteria varies among taxa. In *Escherichia coli*, where RecBCD drives the dominant pathway of recombination by performing the end-resection and RecA loading functions required to initiate HR, RecFOR is relegated to a backup role evident when RecBCD is inactive and the bacterium acquires *sbc* suppressor mutations (11). By contrast, two parallel RecA-dependent HR pathways of recombination operate in *Bacillus subtilis*, one driven by the AddAB

helicase/nuclease (which is homologous to mycobacterial AdnAB) and another by RecFOR. The AddAB and RecFOR pathways contribute equally to clastogen resistance in *Bacillus*, such that both pathways must be inactivated to ablate HR *in vivo* (12). In *Deinococcus radiodurans*, which lacks both RecBCD and AddAB, the RecFOR system constitutes the main pathway of recombinational repair of all DNA breaks, whether single-strand gaps or DSBs (13–15).

The RecO protein of *E. coli* is an essential component of the RecOR and RecFOR recombination mediator complexes that load RecA onto SSB-coated ssDNA (16–19). RecO can also anneal complementary ssDNA protected by its cognate SSB (20–22). Both the RecA loading and single-strand annealing activities of RecO depend on its interaction with the SSB C-terminal peptide (SSB-Ct) (18,22). These RecO functions resemble the activities of yeast Rad52, which mediates loading of Rad51 (the eukaryal RecA homolog) and can anneal complementary ssDNA coated with RPA (the eukaryal SSB) (23,24). In yeast, Rad52 is required for the Rad51-independent single-strand annealing pathway (25), suggesting an *in vivo* role for the annealing activity. However, the *in vivo* function of the single-strand annealing activity of RecO is less clear, as this activity should not be required for RecO to serve as a RecA mediator. Although RecET stimulated illegitimate recombination and plasmid recombination have been demonstrated to be RecO dependent in *E. coli* and appear to involve an SSA type mechanism (26,27), a bonafide SSA pathway that repairs double strand breaks flanked by repeats has not been demonstrated. One suggestion is that *E. coli* RecO might (by analogy to Rad52) promote second-end capture during HR, i.e., the annealing of the processed second DSB end to the single-strand of the D-loop created by RecA-dependent strand invasion (28).

In this study, we examine the function of RecO in mycobacteria. Our results indicate that RecO has dual functions in mycobacterial DSB repair: in a pathway of mycobacterial HR parallel to that mediated by AdnAB, and also in the mycobacterial SSA pathway. Consistent with these dual *in vivo* functions, the biochemical properties of mycobacterial RecO differ from those of the *E. coli* homolog. Mycobacterial RecO displays strong zinc-dependent DNA binding and anneals complementary SSB-coated DNA without interacting physically with the SSB-Ct.

MATERIALS AND METHODS

recO knockout and complementation

In-frame deletion of *Mycobacterium smegmatis recO* in the Δ*adnAB* Δ*recBCD* strain was achieved by a two-step allelic exchange process that uses a suicide vector containing a hygromycin-resistance marker and the counterselectable marker *sacB*, as described previously (1). *recO* was deleted in WT, Δ*adnAB* and Δ*recBCD* backgrounds by specialized transduction using a temperature-sensitive mycobacteriophage. The hyg^R marker (flanked by *loxP* sites) at the disrupted locus was subsequently excised by

expressing Cre recombinase, to generate the unmarked strains Δ*recO*, Δ*recO* Δ*adnAB* and Δ*recO* Δ*recBCD*. Southern blotting was performed to confirm *recO* knockout using either 5′ or 3′ flanking DNA sequence as the probe, and *recBCD* and *adnAB* loci were verified using 5′ and 3′ flanking DNA sequences as the probes, respectively. For complementation, the *M. smegmatis recO* gene along with its 5′ untranslated region (202 bp) containing the presumed promoter was cloned in the mycobacterial integrative vector pMV306kan, to generate pRGM30. The Δ*recO* and Δ*recO* Δ*adnAB* strains were complemented with *recO* by integrating pRGM30 at the *attB* site of the chromosome by plasmid transformation. Rescue of the Δ*recO* mutant phenotypes was tested by assaying clastogen sensitivity. WT, Δ*recO* and Δ*recO* Δ*adnAB* strains harbouring pMV306kan in the chromosomal *attB* locus served as controls in these experiments.

Chromosomal DSB repair assay

Competent *M. smegmatis* cells of the specified genotypes harbouring the chromosomally integrated *lacZ* reporter construct for I-SceI-mediated DSB repair assay (3) were transformed separately with the same molar amount of the I-SceI plasmid and the control vector plasmid to determine the frequency of the DSB repair outcomes and net % survival as described previously (3). For each strain, the experiment was performed at least thrice using different batches of competent cells, and results are expressed as mean values. Among the blue colonies, the gene conversion (GC) and SSA events were distinguished by scoring for kanamycin resistance; kan^R (kanamycin-resistant) colonies represent GC and kan^S (kanamycin-sensitive) colonies denote SSA. Because the % survival values remained constant between different genetic backgrounds, frequencies of different repair outcomes were compared by calculating the relative repair fractions, as follows: relative GC frequency = (GC events/blue events) × (fraction blue); relative SSA frequency = (SSA events/blue events) × (fraction blue).

Growth studies

M. smegmatis strains were revived from frozen glycerol stocks by repeated sub-culturing in LB medium (supplemented with 0.5% glycerol, 0.5% dextrose and 0.1% Tween 80) to ensure that all cells had entered log phase. To study growth kinetics, the strains were re-inoculated into fresh medium to A_{600} of 0.1, incubated at 37°C with constant shaking (150 rpm) and aliquots were removed at regular intervals to measure A_{600} and determine colony forming units (CFUs) by serial-dilution plating. Change in absorbance or CFUs was plotted against time. Doubling times were calculated using the formula: doubling time = time $(t - t_0)$/number of generations (G), where G = (log[#bacteria or A_{600} at time(t)] − log[#bacteria or A_{600} at time(t_0)])/0.301.

Clastogen sensitivity assays

Mycobacterium smegmatis cultures were grown at 37°C in LB medium supplemented with 0.5% glycerol, 0.5% dextrose and 0.1% Tween 80 to log-phase (A_{600} of

0.4–0.5) and subjected to treatment with different DNA-damaging agents, i.e. UV, Methyl methanesulfonate (MMS) and IR as described previously (3). Ten-fold serial dilutions of the treated and untreated cells (derived from the same culture) were then spotted on LB agar plates or LB agar plates containing 20 µg/ml kanamycin (in case of *recO* complementation experiments), and % survival was calculated compared with untreated control cells.

Purification of RecO and SSB

His-tagged *M. smegmatis* RecO (MsRecO) protein was cloned in pMCSG7, and expressed in *E. coli*, and purified using methods described previously for the *Deinococcus radiodurans* and *E. coli* RecO proteins (22). *E. coli* SSB (EcSSB) and a C-terminal truncation SSBΔC EcSSBΔC were purified as described (29). *M. smegmatis* SSB (MsSSB) was expressed from plasmid Pet21b-smegSSB (30), which was modified to introduce a translational stop codon before the polyhistidine tag such that the expressed SSB protein has no affinity tag. *M. smegmatis* SSB was produced in *E. coli* and purified by sequential poly-ethylenimine and ammonium sulfate precipitation steps, followed by heparin affinity and size exclusion chromatography steps (29). The EcSSBΔC expression plasmid was a gift from Dr M. Cox. The purity of all proteins was verified by SDS-PAGE and is shown in Supplementary Figure S2.

DNA and SSB-Ct binding assays

Assay components were prepared as previously described (22). Proteins were dialysed or diluted into buffer A (50 mM NaCl, 25% (v/v) glycerol, 50 mM HEPES pH 7.5, 1 mM Tris(2-carboxyethyl)phosphine (TCEP)), buffer B (100 mM NaCl, 25% glycerol, 20 mM Bis-Tris-Propane, pH 7.5, 1 mM TCEP), buffer C (50 mM NaCl, 25% glycerol, 20 mM Bis-Tris-Propane, pH 7.5, 1 mM TCEP) or buffer D (200 mM NaCl, 25% glycerol, 20 mM Bis-Tris-Propane, pH 7.5, 1 mM TCEP). Protein concentrations were determined by absorbance at 280 nm and with extinction coefficients of $24\,595\,M^{-1}cm^{-1}$ (EcRecO) or $30\,668\,M^{-1}cm^{-1}$ (MsRecO). Lyophilized fluorescein 5′-labelled (FAM) dT_{15} and dT_{35} oligonucleotides were solubilized with Milli-Q H_2O. Double-stranded DNA was generated by mixing FAM-labelled 15mer (5′-T ATCCGCAGAGTTGG) with an equimolar amount of complementary unlabelled 15mer (5′-CCAACTCTGCG GATA) and incubating at 95°C for 1 min, followed by annealing at room temperature for 30 min. FAM-labelled EcSSB-Ct peptide [WMDFDDDIPF (Genscript)] was solubilized with dimethylformamide and diluted into assay buffer; peptide concentration was measured by tryptophan absorbance at 280 nm with an extinction coefficient of $5500\,M^{-1}cm^{-1}$. The concentration of FAM-labelled MsSSB-Ct peptide [GADDEPPF (Lifetein Inc.)] was measured by FAM absorbance at 485 nm using EcSSB-Ct FAM absorption as a reference. Fluorescence anisotropy assays were performed by serially diluting RecO in the indicated buffer with or without $Zn(OAc)_2$. FAM-labelled DNA (5 nM) or SSB-Ct peptide (20 nM) was added to RecO in a final volume of 100 µl and incubated for 30 min. Binding was measured

with excitation/emission of 485/528 nm at room temperature using a BioTek Synergy 2 plate reader. Anisotropy values were normalized using equation: $A = (A_i - A_0)/A_0$, where A_0 and A_i are anisotropy values of free and protein-bound FAM-labelled DNA or SSB-Ct, respectively. Binding constants were calculated using BioKin Dynafit using simple binding equations [RecO]+[DNA or SSB-Ct] <=> [RecO.DNA or SSB-Ct].

DNA annealing assay

RecO-mediated DNA annealing was assayed as described previously (22). SSB concentrations were measured by absorbance at 280 nm and with extinction coefficients of $18\,975\,M^{-1}cm^{-1}$ (EcSSB), $18\,010\,M^{-1}cm^{-1}$ (EcSSBΔC) or $17\,401\,M^{-1}cm^{-1}$ (MsSSB). 49mer 5′-FAM-labelled and complementary 3′-Dabcyl-labelled oligonucleotides at 20 nM were incubated separately with 200 nM of SSB for 30 min at room temperature in buffer D. Complementary oligo•SSB complexes were mixed, and RecO was added and incubated for 30 min at room temperature in the presence or absence of 50 µM $Zn(OAc)_2$. Annealing was measured by a decrease of FAM emission (excitation/emission of 485/528 nm) as a function of time for a total of 21 min. Final annealing amplitude was normalized using equation: $I = -1 \times (I_i - I_0)/I_0$, where I_0 and I_i are intensity values of ssDNA and annealed dsDNA.

RESULTS

recO is not required for *M. smegmatis* viability

Early bioinformatic surveys of the predicted mycobacterial proteome failed to identify RecO (31,32), but later analyses did (33). An alignment of the primary structure of the putative *M. smegmatis* RecO protein (a 280-aa poly-peptide encoded by MSMEG_4491) with the RecO proteins from *D. radiodurans*, *Bacillus subtilis*, *Helicobacter pylori*, *Neisseria gonorrhea* and *E. coli* is shown in Supplementary Figure S1. *M. smegmatis* RecO is 24% identical/38% similar to *E. coli* RecO, 26% identical/46% similar to *B. subtilis* RecO, and 31% identical/47% similar to *D. radiodurans* RecO. Mycobacterial RecO contains a tetracysteine motif (see green boxes in Supplementary Figure S1) that is also found in the RecO proteins from *D. radiodurans* and *B. subtilis*, but not in *E. coli* RecO. *M. smegmatis* RecO is highly conserved among mycobacteria—with homologs in *M. marinum* (83% identical), *M. tuberculosis* (81% identical), *M. intracellulare* (82% identical), *M. leprae* (82% identical), *M. gilvum* (84% identical), *M. avium* (80% identical), *M. abscessus* (83% identical) and *M. bovis* (79% identical). RecO is also conserved in other *Actinomycetales* such as *Rhodococcus equi* (78% identical) and *Nocardia abscessus* (75% identical). Despite the limited amino acid sequence conservation between the *E. coli* and *D. radiodurans* RecO proteins (30% identity), the secondary structural elements of the two proteins, indicated above and below the alignment in Supplementary Figure S1, are well conserved.

To interrogate the role of RecO in mycobacterial DSB repair, we deleted the *recO* gene (MSMEG_4491) from the
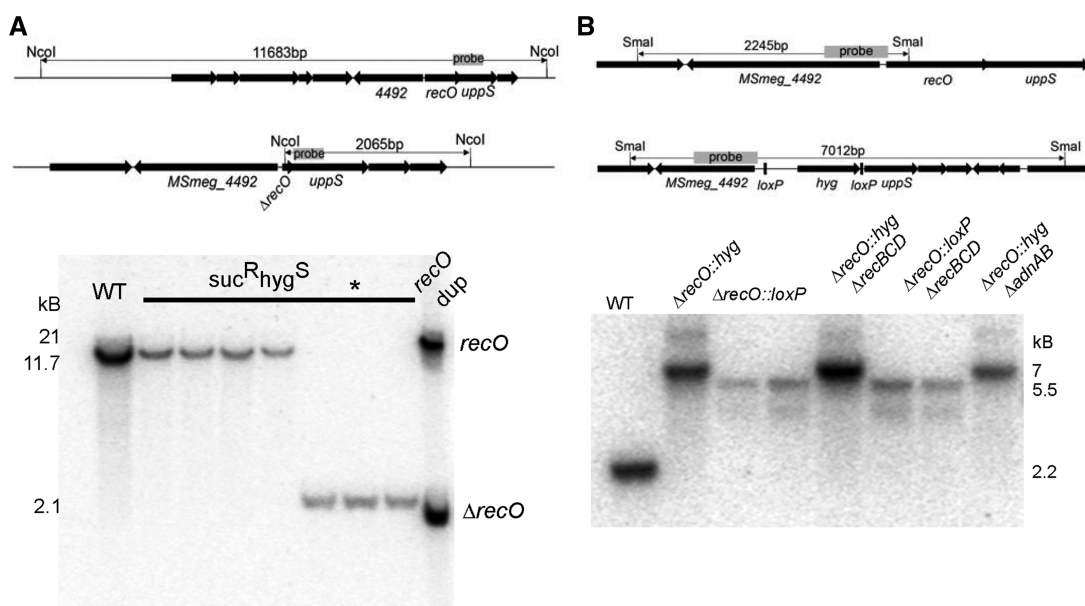
Figure 1. Deletion of *recO* in *Mycobacterium smegmatis*. (**A**) Generation of the Δ*recBCD* Δ*adnAB* Δ*recO* strain by two-step allelic exchange. Map of the wild-type and Δ*recO* loci with NcoI restriction sites, probe location and predicted fragment sizes for WT (11683 bp) and Δ*recO* (2065 bp). Below the restriction maps is a Southern hybridization of chromosomal DNA isolated from Δ*recBCD* Δ*adnAB M. smegmatis* (labelled WT with regard to the *recO* locus), seven sucrose-resistant, hygromycin-sensitive recombinants, and the parental *recO* duplication strain (*recO* dup) which contains the wild-type allele of *recO* and the Δ*recO* deletion allele at the 3′-end of the *recO* locus, separated by the *hyg* and *sacB* markers. The lane marked with the asterisk denotes the strain used for further studies. (**B**) Deletion of *recO* by specialized transduction. Map of the wild-type and Δ*recO*::*loxP*-*hyg*-*loxP* loci with SmaI restriction sites, probe location, and predicted fragment sizes for WT (2245 bp) and Δ*recO*::*loxP*-*hyg*-*loxP* (7012 bp) after SmaI restriction of chromosomal DNA. Below the restriction maps is a Southern hybridization of chromosomal DNA from wild-type *M. smegmatis* (WT), Δ*recO*::*hyg* (lanes 2, 5, 8 in the indicated strain backgrounds) or *recO*::*loxP* (after Cre recombinase-mediated excision of the *hyg* marker, lanes 3, 4, 6, 7).

M. smegmatis chromosome by allelic exchange. To interrogate potential epistatic relationships between *recO* and the *adnAB*-dependent HR and *recBCD*-dependent SSA pathways, the Δ*recO* allele was also introduced into the Δ*adnAB*, Δ*recBCD*, and Δ*adnAB* Δ*recBCD* strains. The strategy for genotyping by Southern blotting depicted in Figure 1A demonstrates the deletion of *recO* in the Δ*adnAB* Δ*recBCD* strain background, leaving an unmarked Δ*recO* allele. Specialized transduction of a Δ*recO*::*loxP*-*hyg*-*loxP* allele was used to delete *recO* in the three other strain backgrounds (Figure 1B). The hygromycin-resistance cassette was then excised using the Cre recombinase to yield unmarked Δ*recO*, Δ*recO* Δ*adnAB*, and Δ*recO* Δ*recBCD* mutants (Figure 1B). The presence of the Δ*recBCD* and Δ*adnAB* alleles was confirmed by diagnostic Southern blotting (data not shown).

Δ*recO* strains have diminished growth rate

We examined the growth characteristics of Δ*recO* strains by measuring A_{600} in logarithmic cultures and comparing these cell density measurements to the number of viable bacteria. The apparent doubling times of the Δ*recO* mutants were determined after repeated serial dilution of logarithmic phase cultures. In comparison to wild type (doubling time 174 min), the Δ*recO* (212 min) and Δ*recO* Δ*adnAB* (231 min) strains grew slower and their growth rates were similar to that observed for the Δ*recA* strain (226 min). This difference in apparent doubling time

was not the result of altered cell shape, as the doubling times of Δ*recO* (215 min), Δ*recO* Δ*adnAB* (222 min) and Δ*recA* (213 min) calculated from determination of viable bacteria were greater than that of the wild type strain (155 min). The slow growth phenotype of the mutant strains is also manifest as small colony size when cultured on agar media (Figure 2B).

RecO is required for survival upon DNA damage

Our previous results indicated that the *M. smegmatis* Δ*adnAB* strain is sensitized to killing by diverse clastogens, whereas Δ*recBCD* cells are not (3). However, the Δ*adnAB* strain is less sensitive to DNA damage than a Δ*recA* strain, indicating that there are AdnAB-independent pathways of homology-directed repair. To investigate if RecO is involved in DNA repair in mycobacteria, we studied the survival of the Δ*recO* strains after exposure to UV, IR and the alkylating agent MMS. The deletion of *recO* conferred severe sensitivity to UV radiation (Figure 2A), ionizing radiation (Figure 2B) and MMS (Figure 2C). The clastogen sensitivity of the Δ*recO* strain was indistinguishable from Δ*recA* (Figures 2A–C). Note that the Δ*recO* Δ*adnAB*, Δ*recO* Δ*recBCD* and Δ*recO* Δ*adnAB* Δ*recBCD* strains were no more sensitive to UV, IR or MMS than the Δ*recO* strain (Figure 2, Supplementary Figure S2). These results suggest that RecO and RecA function in the same pathway of DNA repair, conceivably by loading RecA onto single-stranded DNA at damage sites.
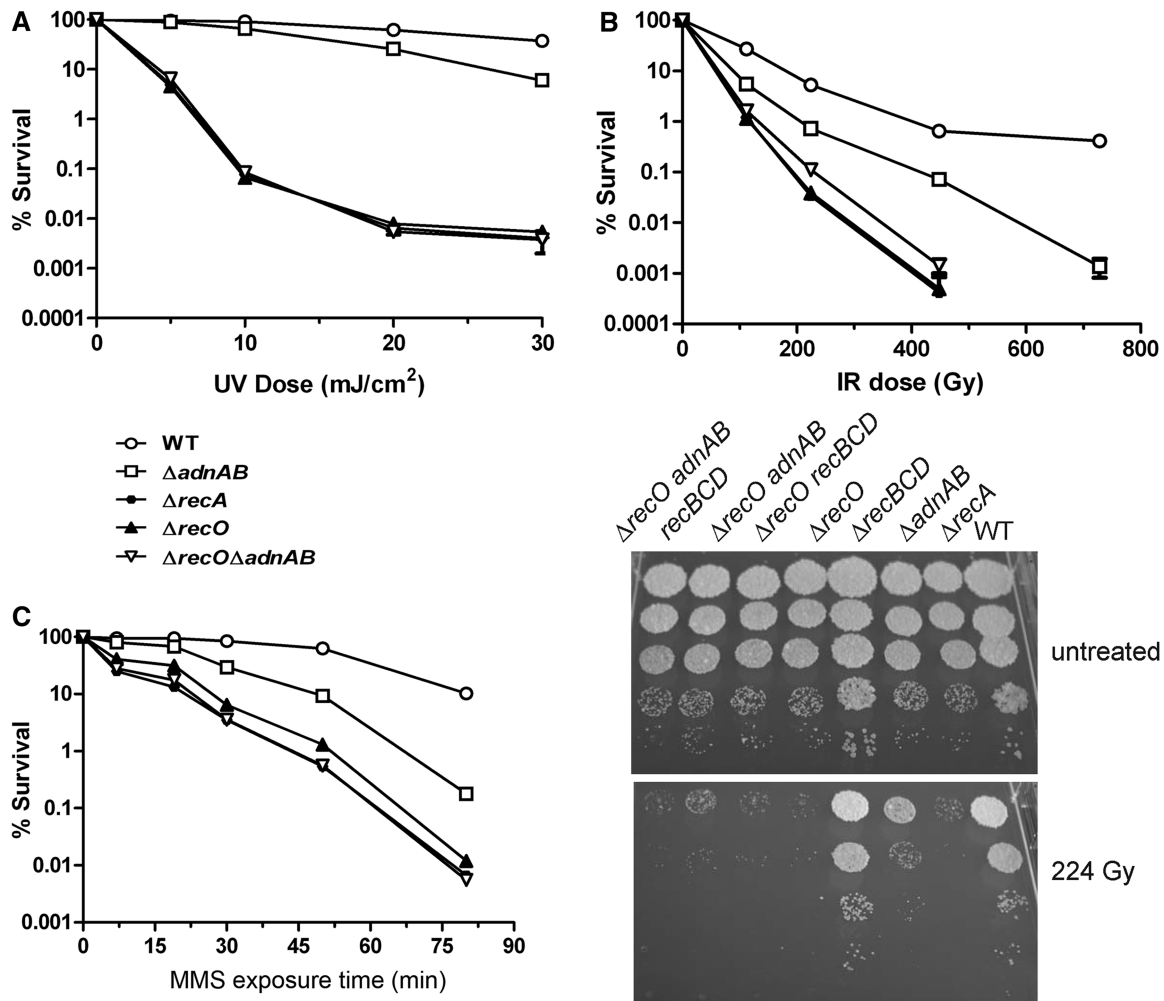
Figure 2. Δ*recO* phenocopies Δ*recA* in clastogen resistance. (**A**) Survival curves of WT *M. smegmatis* (open circle), Δ*adnAB* (open square), Δ*recA* (filled circle), Δ*recO* (filled triangle), Δ*recO* Δ*adnAB* (inverted open triangle) exposed to escalating doses of UV light. Survival is plotted on a log scale and is calculated compared with an unexposed control for each strain. (**B**) Ionizing radiation survival curve using the same strain key as in panel A. The plate pictures below the graph are a representative unexposed (top panel) and 224 Gy exposed (bottom panel) 10-fold dilutions of the indicated strains. (**C**) MMS-induced killing. The *x*-axis represents the time of MMS exposure and survival is plotted on a log scale on the *y*-axis.

In the *M. smegmatis* chromosome, the *recO* gene appears to be in an operon with three other genes, namely MSMEG_4490 (*uppS*, encoding undecaprenyl diphosphate synthase), MSMEG_4489 (encoding a conserved hypothetical protein) and MSMEG_4488 (encoding a nudix family hydrolase) (Figure 1). The predicted translational start codon of *uppS* overlaps the 3′-end of *recO* by 53 nucleotides, raising the possibility that the *recO* deletion in our strains might disrupt *uppS* expression. Although we were careful to leave the coding sequence of *uppS* intact, we performed a complementation experiment to confirm that the clastogen sensitivity of our Δ*recO* strain was due to loss of RecO function. Complementation of the deletion mutant with a single *recO* copy at the phage L5 integration site in the chromosome restored the clastogen resistance of the Δ*recO* strain to wild-type levels (Figure 3A and B). Complementation of the Δ*recO* Δ*adnAB* strain with *recO* restored the clastogen resistance to the level of the Δ*adnAB* strain (Figure 3). Together, these results verify that the

phenotype of the *recO* deletion is due to loss of *recO* and not due to a polar effect in the *recO* operon or a spontaneous mutation elsewhere in the chromosome.

RecO participates in a parallel pathway to AdnAB in RecA-dependent HR

Because UV, IR and MMS produce diverse types of DNA damage, the clastogen sensitivity of the *recO* mutant does not suffice for conclusions about the function of *recO* in specific pathways of DNA repair. To interrogate the participation of RecO in DSB repair, we used an I-SceI recombination system developed previously (3). In this system, a recombination substrate is integrated into the chromosome of *M. smegmatis* at the L5 phage attachment site. This recombination substrate contains two defective *lacZ* alleles, *lacZ*-I-SceI and *lacZ*-ΔN, which are separated by a kanamycin-resistance cassette. *lacZ*-I-SceI is interrupted by two recognition sites for the homing endonuclease I-SceI such that cleavage by I-SceI
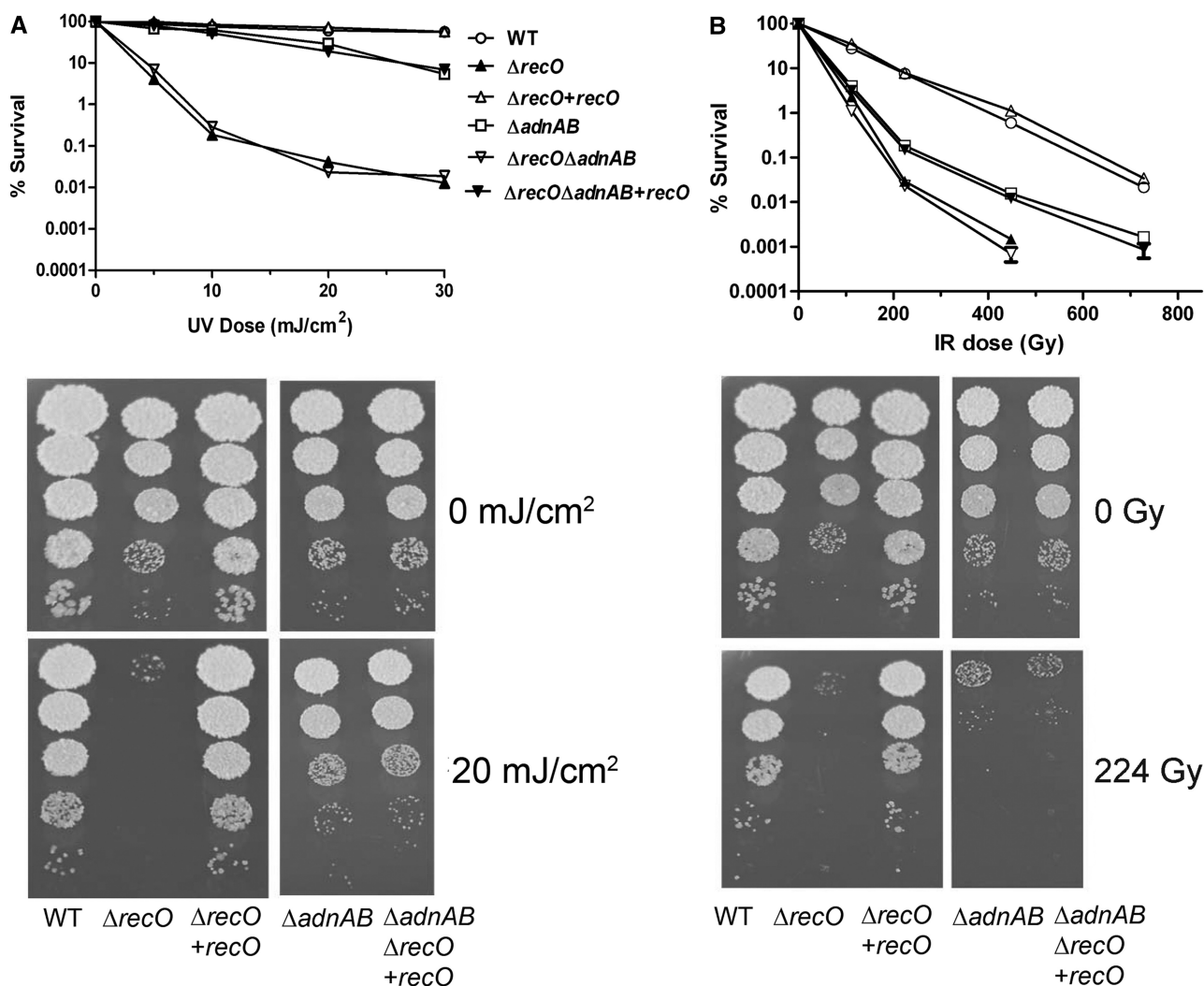
Figure 3. The clastogen susceptibility of the $\Delta recO$ strain is due to loss of *recO*. (**A**) Survival curves of WT *M. smegmatis* (open circle), $\Delta adnAB$ (open square), $\Delta recO$ (filled triangle), $\Delta recO$ $\Delta adnAB$ (inverted open triangle), $\Delta recO$ $\Delta adnAB$ complemented with a single copy of *recO* (inverted triangle), or $\Delta recO$ complemented with a single copy of *recO* (open triangle) exposed to escalating doses of UV light. Survival is plotted on a log scale and is calculated compared to an unexposed control for each strain. The plate pictures below the graph show unexposed and $20\,mJ/cm^2$ exposed 10-fold serial dilutions of the indicated strains. (**B**) Survival curves of the same strains as in (A) exposed to escalating doses of ionizing radiation. Survival is plotted on a log scale and is calculated compared to an unexposed control for each strain. The plate pictures below the graph show unexposed and 224 Gy-exposed 10-fold serial dilutions of the indicated strains.

produces a chromosomal break with incompatible 3′ overhangs. Repair of this break can be achieved by three mechanisms: NHEJ, gene conversion (GC) or SSA (Figure 4A). NHEJ (which requires *ku* and *ligD*) ligates the broken ends after varying degrees of end-resection and end-healing, and therefore does not reconstitute an active *lacZ* gene. Thus, repair via NHEJ yields a white colony that is kanamycin-resistant in most cases, unless an especially long end-resection invades the kanamycin-resistance gene. GC (which is *recA*-dependent) uses the downstream *lacZ*-ΔN as a homologous template to repair the DSB. This mechanism of repair reconstitutes a functional *lacZ* gene while leaving the kanamycin-resistance cassette intact, yielding a blue, kanamycin-resistant colony. Finally, repair by SSA (which is *recBCD*-dependent) results from bidirectional single-strand resection from the I-SceI sites, revealing complementary single strands

that can anneal and reconstitute an intact *lacZ* allele with a deletion that eliminates the kanamycin-resistance marker. Thus, all three repair outcomes can be scored on agar plates containing X-gal and counterscreening for kanamycin resistance, as depicted in Figure 4A. Repair by SSA and GC is then confirmed by diagnostic PCR amplification (3).

We applied this system to understand the function of RecO in DSB repair. Induction of a DSB by transformation of an I-SceI encoding plasmid in wild-type cells yields an approximate 50:50 mixture of white and blue colonies, as reported previously (3). Of these blue colonies, 80% are GC (40% of the total outcomes) and 20% are SSA (10% of the total) (Figure 4B–E). In the $\Delta recO$ strain, we observed a 5-fold decrement in the yield of blue colonies after I-SceI transformation (Figure 4B and E). Testing kanamycin resistance and
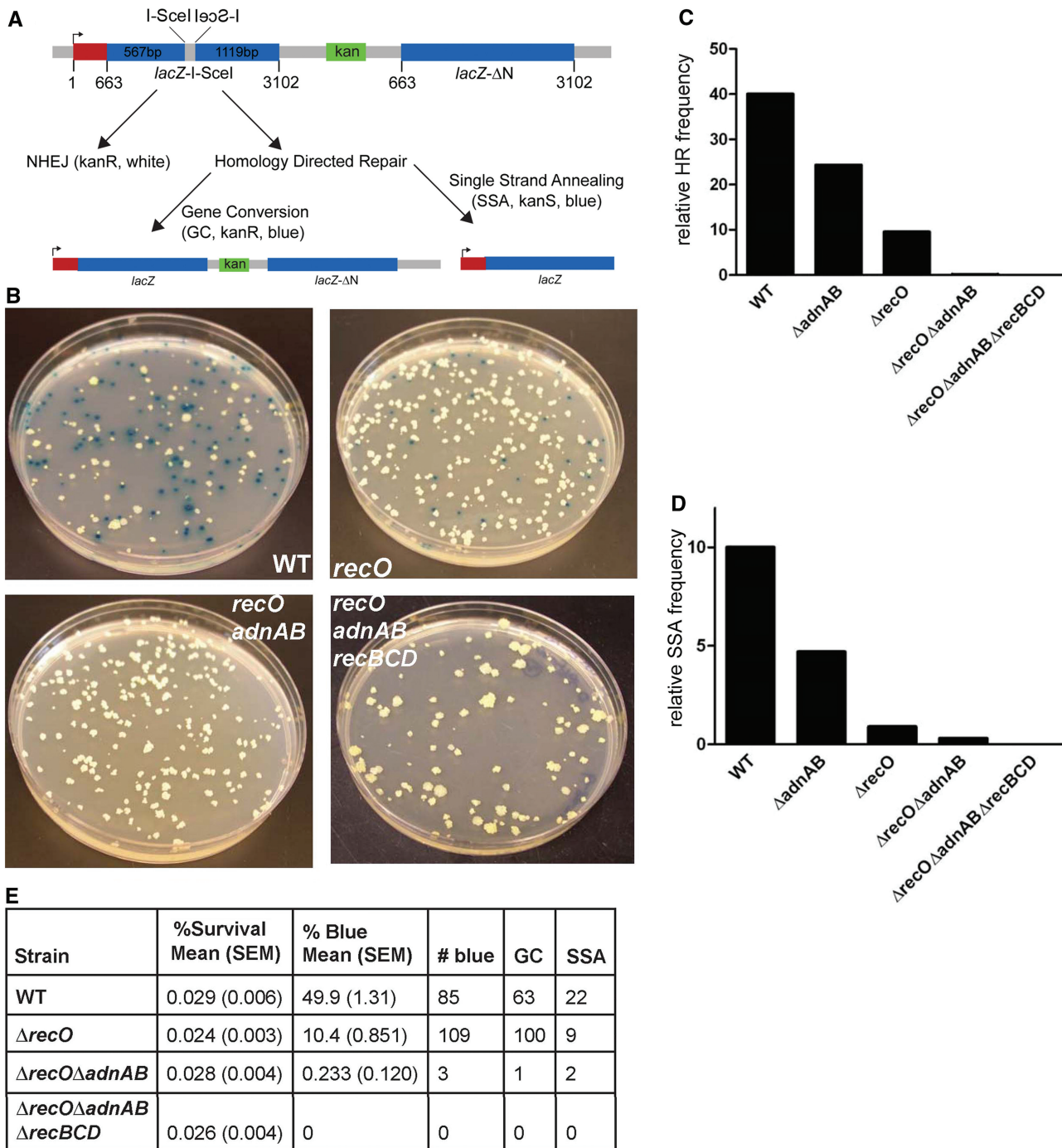
Figure 4. RecO is required for *adnAB*-independent GC and SSA. (**A**) Schematic of DSB repair outcomes in the I-SceI system, adapted from (3). An I-SceI-induced DSB is initiated by transformation of a plasmid encoding I-SceI into a strain bearing a previously described I-SceI recombination substrate. Repair of this incompatible DSB yields either blue or white colonies. White colonies can result either from NHEJ-mediated repair, or inactivation of the I-SceI enzyme through mutation. Blue colonies indicate that the defective *lacZ* coding sequence has been restored either through SSA or GC. DNA resection that occurs during SSA results in deletion of the kanamycin marker, whereas GC does not. (**B**) Each panel shows *M. smegmatis* of the indicated genotype transformed with the I-SceI encoding plasmid and cultured on agar plates containing hygromycin and X-gal. (**C**) Graph of GC frequency according to strain genotype. For each strain, the relative GC frequency is calculated from the genotyping algorithm in (A) and the raw data presented in the table in (E). The graphed Δ*adnAB* data is from (3). (**D**) SSA frequency for the strains indicated. The graphed Δ*adnAB* data is from (3). (**E**) Survival, % blue and pathway outcome for each strain. #blue is the number of blue colonies genotyped to give the GC and SSA numbers. Relative GC frequency is given as (%blue) (#GC/#blue). SSA frequency is given as (%blue) (#SSA/#blue).

genotyping the blue colonies indicated that gene conversion outcomes were 4-fold less frequent than in wild-type cells (relative GC frequency in WT versus $\Delta recO$, 37% versus 9.5%), compared with the 2-fold decrement observed in the $\Delta adnAB$ strain in our prior study (3). We then examined the GC frequency in the $\Delta adnAB$ $\Delta recO$ double mutant and observed a near complete abolition of GC outcomes (relative GC frequency in $\Delta adnAB$ $\Delta recO = 0.077\%$). These data indicate that $adnAB$ and $recO$ define parallel pathways of $recA$-dependent gene conversion.

Requirement for RecO in the RecBCD-dependent SSA pathway

We next examined the role of RecO in the mycobacterial SSA pathway. In wild-type cells, SSA outcomes accounted for 26% of the blue colonies and 12.9% of the total outcomes (Figure 4D and E). In the $\Delta recO$ strain, we observed a 15-fold decrement in SSA outcomes (relative SSA frequency in $\Delta recO = 0.86\%$), compared with the complete loss (0/120) of SSA previously observed in the $\Delta recBCD$ strain. As predicted, there were no blue colonies in the $\Delta recO$ $\Delta recBCD$ $\Delta adnAB$ strain, consistent with the loss of both GC and SSA pathways (Figure 4E). These assays reveal a genetic requirement for the RecO protein in the mycobacterial SSA pathway.

DNA binding by mycobacterial RecO is stimulated by zinc

The genetic data indicate a role for mycobacterial RecO in RecA-dependent GC and in SSA, dual functions not reported previously for RecO proteins. To correlate these *in vivo* roles with the biochemical properties of the mycobacterial RecO protein, we produced His-tagged *M. smegmatis* RecO in *E. coli* and purified it by nickel affinity chromatography (Supplementary Figure S3). We first examined the interaction of RecO with single-stranded DNA under equilibrium conditions by fluorescent anisotropy. Initial experiments revealed a strong dependence of the MsRecO interaction with ssDNA on the presence of zinc. In buffer A with 50 mM NaCl, MsRecO interacted weakly with ssDNA with an apparent dissociation constant (K_d) of $>5 \mu M$ (Figure 5A). *E. coli* RecO (EcRecO) had a noticeably stronger affinity to ssDNA with an apparent K_d of 0.45 (± 0.11) μM (Figure 5A). However, addition of 10 μM $Zn(OAc)_2$ significantly stimulated MsRecO binding to ssDNA with a K_d of MsRecO was 0.036 (± 0.004) μM. In contrast, zinc had no or a slightly inhibitory effect on binding of EcRecO to ssDNA (Figure 5A). Previously, we demonstrated a strong inhibitory effect of increased salt concentration on DNA binding by EcRecO (22). Consistent with these prior results, EcRecO did not appreciably bind ssDNA at 100 mM NaCl, whereas MsRecO
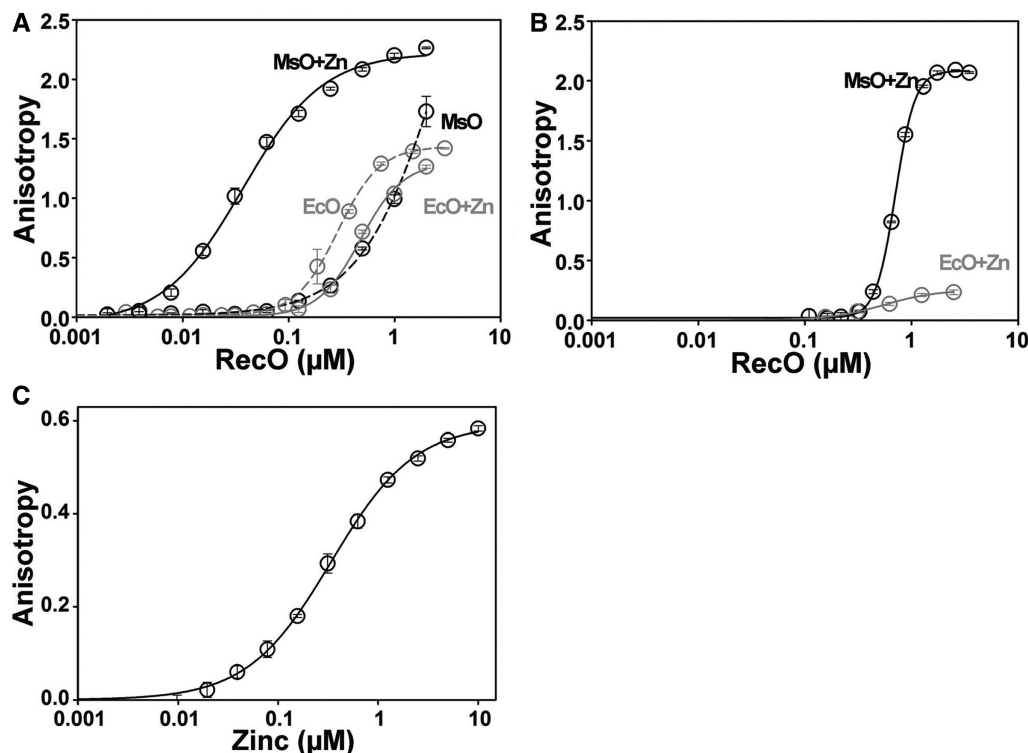
Figure 5. MsRecO binding to ssDNA is stimulated by zinc. (**A**) Equilibrium binding isotherms as measured by fluorescence anisotropy of FAM-dT15 (5 nM) upon titration by MsRecO in buffer A (25% glycerol, 50 mM NaCl, 50 mM HEPES pH 7.5, 1 mM TCEP) without $Zn(OAc)_2$ (black dashed lines) and in the presence of 10 μM $Zn(OAc)_2$ (black solid lines). Titration by EcRecO in buffer A without $Zn(OAc)_2$ (gray dashed lines) and in the presence of 10 μM $Zn(OAc)_2$ (gray solid lines). (**B**) Anisotropy of FAM-dT15 (5 nM) upon titration by MsRecO (black) and EcRecO (grey) in buffer B (Buffer A with 100 mM NaCl) in the presence of 50 μM $Zn(OAc)_2$. (**C**) Anisotropy of FAM-dT15 (5 nM) in the presence of MsRecO (500 nM) upon titration by $Zn(OAc)_2$ in buffer A.

retained strong interaction with ssDNA in the presence of 100 mM NaCl plus Zn(OAc)$_2$ with K_d of 1 (± 0.03) μM (Figure 5B). Magnesium did not stimulate DNA binding (data not shown). We also found that MsRecO bound dsDNA with equivalent affinity to ssDNA of the same length (Supplementary Figure S4). These results indicate that mycobacterial RecO binds ssDNA more avidly than *E. coli* RecO at moderate ionic strength and that this DNA binding is zinc-dependent.

The zinc requirement for DNA binding can be attributed to the presence of the 4xCys zinc-binding motif in the MsRecO primary structure (Supplementary Figure S1), similar to that of *D. radiodurans* RecO (DrRecO). DrRecO binds Zn^{2+} with sufficient affinity to carry the bound ion through multiple purification and crystallization steps involving the use of zinc-free solutions (34). The requirement for exogenous Zn^{2+} for MsRecO to bind DNA possibly indicates weaker interaction with the metal ion. We used an ssDNA-binding assay to measure Zn^{2+} binding by MsRecO. The K_d of MsRecO for Zn^{2+} was estimated to be 0.15 (± 0.001) μM (Figure 5C). Therefore, interaction of MsRecO with DNA is modulated by the presence of micromolar concentrations of zinc ion, which might serve as a regulator of RecO DNA binding *in vivo*.

Mycobacterial RecO does not interact with C-terminal tail of SSB

SSB exhibits one of the highest affinities for ssDNA of any protein and is critical for protecting it from nucleases and for mediating interactions with other DNA-binding proteins (35). The majority of such interactions are mediated by a conserved C-terminal tail of SSB (SSB-Ct), which is essential for the viability of *E. coli* (36). Interaction of EcRecO with the conserved hydrophobic residues of SSB-Ct is important for binding of RecO to SSB-coated ssDNA and DNA annealing at moderate salt concentrations (22) as well as for loading of RecA by RecOR (18). However, this SSB-Ct binding is not conserved among all RecO proteins. For example, the SSB-Ct binding site is not conserved in DrRecO, which also contains a 4xCys zinc-binding motif, similar to MsRecO. We therefore sought to determine whether MsRecO interacts with either *E. coli* SSB-Ct or mycobacterial SSB-Ct and to interrogate the requirement for the RecO•SSB-Ct interaction for RecO function. An alignment of the SSB C-termini from *E. coli* and *M. smegmatis* is shown in Figure 6A. In comparison to the *E. coli* peptide, the *M. smegmatis* peptide is two amino acids shorter and differs by substitution of a proline in place of isoleucine in third position from the C-terminus and glutamate substituting aspartate in the adjacent position.

We measured the strength of the RecO/SSB-Ct interaction by anisotropy of a fluorescein-labelled peptide composed of the C-terminal amino acids of *E. coli* SSB (FAM-WMDFDDDIPF) or *M. smegmatis* SSB (FAM-GADDEPPF). MsRecO did not bind SSB-Ct either from *E. coli* or *M. smegmatis* ($K_d > 10 \mu$M, Figure 6B) regardless of whether zinc was present. EcRecO interacted
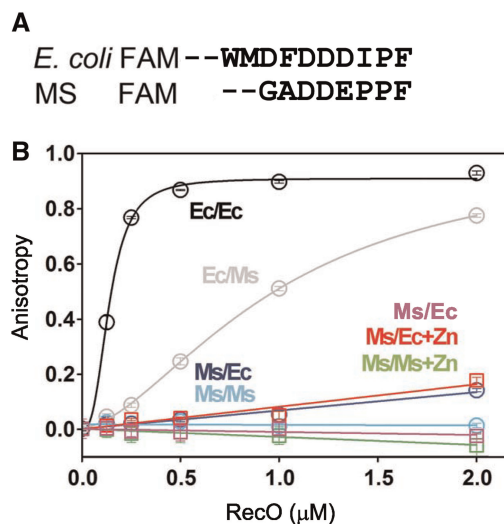
Figure 6. MsRecO does not bind SSB-Ct. (**A**) Sequence of the *E. coli* SSB and the *M. smegmatis* SSB C-terminal peptide FAM conjugates. (**B**) Anisotropy of FAM-MsSSB-Ct (20 nM) and FAM-EcSSB-Ct (20 nM) upon titration by EcRecO (gray and black circles, respectively) or by MsRecO (cyan and blue circles, respectively) in buffer A. Anisotropy of FAM-EcSSB-Ct (20 nM) titrated by MsRecO in the absence (magenta squares) or presence of 10 μM Zn(OAc)$_2$ (red squares) and of MsSSB-Ct in the presence of 10 μM Zn(OAc)$_2$ (green squares) in buffer C (200 mM NaCl). Labels correspond to RecO/SSB-Ct.

with both peptides, albeit with lower affinity for MsSSB-Ct (K_d of 3.0 μM) compared with EcSSB-Ct (K_d of 0.12 μM) (Figure 6B). The lack of interaction between MsRecO and MsSSB-Ct raises questions about whether and how mycobacterial RecO can bind ssDNA when SSB is present.

Mycobacterial RecO can anneal SSBΔC-coated ssDNA

The Δ*recO M. smegmatis* strain is defective for DSB repair via the SSA pathway (Figure 4), which suggests that MsRecO may aid in annealing SSB-coated DNA at resected DSB ends. In *E. coli*, annealing of ssDNA by RecO requires the hydrophobic interaction between RecO and the SSB-Ct at moderate salt concentration (22). We investigated the ability of EcRecO and MsRecO to anneal SSB-coated complementary single-strand DNAs using a fluorescence quenching annealing MsSSB-coated ssDNA (Figure 7). This annealing activity was abolished when truncated EcSSBΔC was included in the reaction in lieu of full length SSB (Figure 7A and B), indicating that the annealing activity of EcRecO depends on interaction with the SSB-Ct. MsRecO also promoted annealing of ssDNA coated with either EcSSB or MsSSB when Zn^{2+} was present in the annealing reaction. However, in contrast to EcRecO, the annealing activity of MsRecO was unaffected by deletion of the SSB-Ct (Figure 7). Therefore, mycobacterial RecO is able to anneal complementary SSB-coated DNA strands independent of an interaction with the SSB-Ct.
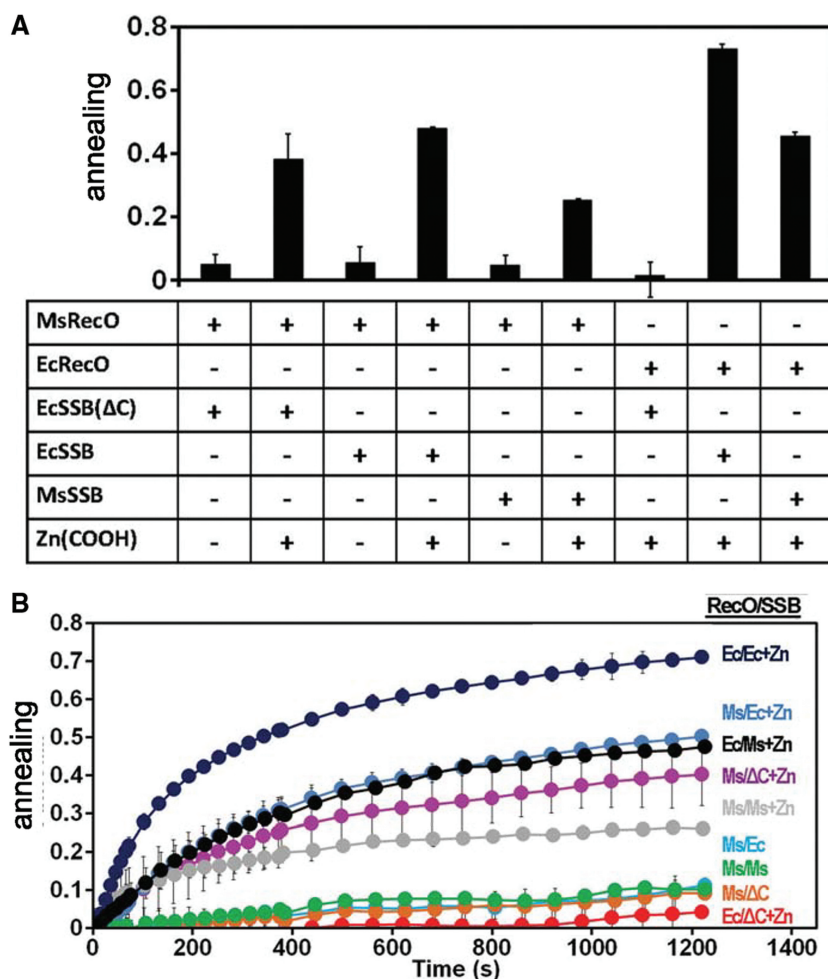
Figure 7. MsRecO anneals SSB-coated DNA at moderate salt without interacting with the SSB C-terminus. (**A**) Relative degree of FAM quenching corresponding to annealing of FAM-labelled 49mer ssDNA and Dabcyl-labelled 49mer complementary ssDNA (20 nM) after 21 min. Each strand was incubated separately with either full length or truncated *E. coli* SSB or full length *M. smegmatis* SSB (200 nM). After 30 min, strands were mixed and RecO was added (2 μM). All reactions were performed in buffer D. Proteins and presence of 50 μM $Zn(OAc)_2$ in each reaction are shown below bar graph. (**B**) Time course of annealing using the indicated combinations of *E. coli* or *M. smegmatis* RecO/SSB, with or without zinc, as indicated to the right of each annealing curve.

DISCUSSION

We have examined the genetic and biochemical functions of mycobacterial RecO and found dual *in vivo* functions in the HR and SSA pathways. The critical role of RecO in the RecA-dependent recombination pathway is clearly distinct from the function of RecO in *E. coli*, but similar to *B. subtilis*, in which the RecFOR system has an important role in recombination in wild-type cells. Our studies also clearly indicate a RecO-independent, AdnAB-dependent HR pathway. The genetic requirement for RecO in the mycobacterial HR pathway may reflect a RecA loading function of RecO in association with RecF and/or RecR. This model is based on the function of the RecFOR complex in *E. coli* as a RecA mediator (16). Alternatively, the RecO protein may be required not for RecA loading, but rather for second-end capture via its annealing activity, as documented for yeast Rad52 (28).

Our studies indicate that mycobacterial RecO differs from *E. coli* RecO in its interaction with SSB.

Mycobacterial RecO does not interact directly with the SSB C-terminal tail. It has been reported that the mycobacterial SSB C-terminal tail interacts directly with RecA both *in vitro* and *in vivo* (37), an interaction not described for other bacterial RecA proteins (35,38). This direct interaction between SSB-Ct and RecA may suggest that RecO is not needed for recruitment of RecA to SSB-coated ssDNA. We predict that if RecO functions as a mediator for mycobacterial RecA, then the role of RecO would not be to recruit RecA to SSB-coated DNA, but rather to facilitate RecA/SSB exchange. Alternatively, the direct recruitment of RecA by the SSB-Ct may reflect a fundamentally different mechanism of RecA loading in mycobacteria that may not require RecO.

Multiple other components of the two parallel pathways of recombination in mycobacteria remain to be identified. For the RecO pathway, the nuclease that resects the DSB before RecO action is unknown. In the RecFOR systems of other bacteria, RecJ performs this function (16,39). However, no RecJ exonuclease has been identified in

mycobacteria, leaving the identity of the resection nuclease in the mycobacterial RecO pathway obscure.

Our prior results indicated that mycobacteria have an SSA pathway that depends on RecBCD (3). In this work we implicate the RecO protein in the SSA pathway. RecO proteins are known to exhibit single-strand annealing activity. However, the *in vivo* function of this annealing activity has not been demonstrated. It has been suggested that this annealing activity may catalyse the annealing of the second resected end onto the displaced D-loop created by strand invasion during RecA-dependent HR (28). However, this model was based on bacteria that do not apparently encode an SSA pathway of DSB repair. Our data suggest an additional *in vivo* function for the DNA annealing activity of RecO in the annealing of single-stranded DNA during repair by the SSA pathway. This function of RecO in mycobacteria echoes that of yeast Rad52, which also anneals single-stranded DNA and is genetically required for both the gene conversion and SSA pathways (25).

Our biochemical characterization of mycobacterial RecO indicates that the protein is adept at DNA annealing. Mycobacterial RecO binds single-stranded DNA more avidly than *E. coli* RecO. This high-affinity DNA binding might allow mycobacterial RecO to anneal SSB-coated single-stranded DNA without interacting with the SSB C-terminal tail, an interaction that is required for the annealing activity of *E. coli* RecO. MsRecO DNA binding and annealing activities are dependent on added Zn^{2+}, a requirement that is likely due to the tetracysteine zinc-binding motif found in some RecO orthologs but not *E. coli* RecO. It is tempting to speculate that there is a correlation between the presence of a tetracysteine zinc-binding motif in RecO and a lack of binding to the SSB-Ct, because MsRecO and DrRecO share these features. *B. subtilis* RecO possesses a similar 4xCys motif, can compete for DNA binding with SsbA and SsbB (40), and can anneal ssDNA in the presence of SsbA (41), which contains a conserved SSB-Ct. However, the requirement for the SsbA C-terminus in this process has not been examined (41,42). An alternate possibility is that mycobacterial RecO may interact with a region of SSB distinct from the C-terminus, such that its DNA annealing activity still relies on interaction with SSB but via a distinct mechanism.

In summary, our data document a dual function of mycobacterial RecO in two pathways of homology-directed DNA repair. Further biochemical characterization of the RecO–SSB interaction and investigation of the ability of RecO to load RecA onto ssDNA will elucidate the biochemical function of RecO during HR. In addition, separation of function mutations that ablate RecO annealing activity will be useful to understand the novel requirement for RecO in the SSA pathway documented here.

SUPPLEMENTARY DATA

Supplementary Data are available at NAR Online: Supplementary Figures 1–4.

REFERENCES

1. Gong,C., Bongiorno,P., Martins,A., Stephanou,N.C., Zhu,H., Shuman,S. and Glickman,M.S. (2005) Mechanism of nonhomologous end-joining in mycobacteria: a low-fidelity repair system driven by Ku, ligase D and ligase C. *Nat. Struct. Mol. Biol.*, **12**, 304–312.
2. Gong,C., Martins,A., Bongiorno,P., Glickman,M. and Shuman,S. (2004) Biochemical and genetic analysis of the four DNA ligases of mycobacteria. *J. Biol. Chem.*, **279**, 20594–20606.
3. Gupta,R., Barkan,D., Redelman-Sidi,G., Shuman,S. and Glickman,M.S. (2011) Mycobacteria exploit three genetically distinct DNA double-strand break repair pathways. *Mol. Microbiol.*, **79**, 316–330.
4. Shuman,S. and Glickman,M.S. (2007) Bacterial DNA repair by non-homologous end joining. *Nat. Rev. Microbiol.*, **5**, 852–861.
5. Pitcher,R.S., Green,A.J., Brzostek,A., Korycka-Machala,M., Dziadek,J. and Doherty,A.J. (2007) NHEJ protects mycobacteria in stationary phase against the harmful effects of desiccation. *DNA Repair (Amst)*, **6**, 1271–1276.
6. Stephanou,N.C., Gao,F., Bongiorno,P., Ehrt,S., Schnappinger,D., Shuman,S. and Glickman,M.S. (2007) Mycobacterial nonhomologous end joining mediates mutagenic repair of chromosomal double-strand DNA breaks. *J. Bacteriol.*, **189**, 5237–5246.
7. Aniukwu,J., Glickman,M.S. and Shuman,S. (2008) The pathways and outcomes of mycobacterial NHEJ depend on the structure of the broken DNA ends. *Genes Dev.*, **22**, 512–527.
8. Courcelle,J., Carswell-Crumpton,C. and Hanawalt,P.C. (1997) recF and recR are required for the resumption of replication at DNA replication forks in Escherichia coli. *Proc. Natl Acad. Sci. USA*, **94**, 3714–3719.
9. Xu,L. and Marians,K.J. (2003) PriA mediates DNA replication pathway choice at recombination intermediates. *Mol. Cell*, **11**, 817–826.
10. Cox,M.M., Goodman,M.F., Kreuzer,K.N., Sherratt,D.J., Sandler,S.J. and Marians,K.J. (2000) The importance of repairing stalled replication forks. *Nature*, **404**, 37–41.
11. Bidnenko,V., Seigneur,M., Penel-Colin,M., Bouton,M.F., Dusko Ehrlich,S. and Michel,B. (1999) sbcB sbcC null mutations allow RecF-mediated repair of arrested replication forks in rep recBC mutants. *Mol. Microbiol.*, **33**, 846–857.
12. Fernandez,S., Kobayashi,Y., Ogasawara,N. and Alonso,J.C. (1999) Analysis of the *Bacillus subtilis* recO gene: RecO forms part of the RecFLOR function. *Mol. Gen. Genet.*, **261**, 567–573.
13. Bentchikou,E., Servant,P., Coste,G. and Sommer,S. (2010) A major role of the RecFOR pathway in DNA double-strand-break repair through ESDSA in *Deinococcus radiodurans*. *PLoS Genet.*, **6**, e1000774.
14. Satoh,K., Kikuchi,M., Ishaque,A.M., Ohba,H., Yamada,M., Tejima,K., Onodera,T. and Narumi,I. (2012) The role of *Deinococcus radiodurans* RecFOR proteins in homologous recombination. *DNA Repair (Amst)*, **11**, 410–418.
15. Xu,G., Wang,L., Chen,H., Lu,H., Ying,N., Tian,B. and Hua,Y. (2008) RecO is essential for DNA damage repair in *Deinococcus radiodurans*. *J. Bacteriol.*, **190**, 2624–2628.
16. Handa,N., Morimatsu,K., Lovett,S.T. and Kowalczykowski,S.C. (2009) Reconstitution of initial steps of dsDNA break repair by the RecF pathway of E. coli. *Genes Dev.*, **23**, 1234–1245.
17. Morimatsu,K. and Kowalczykowski,S.C. (2003) RecFOR proteins load RecA protein onto gapped DNA to accelerate DNA strand

exchange: a universal step of recombinational repair. *Mol. Cell*, **11**, 1337–1347.

18. Sakai,A. and Cox,M.M. (2009) RecFOR and RecOR as distinct RecA loading pathways. *J. Biol. Chem.*, **284**, 3264–3272.

19. Sandler,S.J. and Clark,A.J. (1994) RecOR suppression of recF mutant phenotypes in *Escherichia coli* K-12. *J. Bacteriol.*, **176**, 3661–3672.

20. Umezu,K., Chi,N.W. and Kolodner,R.D. (1993) Biochemical interaction of the *Escherichia coli* RecF, RecO, and RecR proteins with RecA protein and single-stranded DNA binding protein. *Proc. Natl Acad. Sci. USA*, **90**, 3875–3879.

21. Kantake,N., Madiraju,M.V., Sugiyama,T. and Kowalczykowski,S.C. (2002) *Escherichia coli* RecO protein anneals ssDNA complexed with its cognate ssDNA-binding protein: a common step in genetic recombination. *Proc. Natl Acad. Sci. USA*, **99**, 15327–15332.

22. Ryzhikov,M., Koroleva,O., Postnov,D., Tran,A. and Korolev,S. (2011) Mechanism of RecO recruitment to DNA by single-stranded DNA binding protein. *Nucleic Acids Res.*, **39**, 6305–6314.

23. New,J.H., Sugiyama,T., Zaitseva,E. and Kowalczykowski,S.C. (1998) Rad52 protein stimulates DNA strand exchange by Rad51 and replication protein A. *Nature*, **391**, 407–410.

24. Sugiyama,T., New,J.H. and Kowalczykowski,S.C. (1998) DNA annealing by RAD52 protein is stimulated by specific interaction with the complex of replication protein A and single-stranded DNA. *Proc. Natl Acad. Sci. USA*, **95**, 6049–6054.

25. Ivanov,E.L., Sugawara,N., Fishman-Lobell,J. and Haber,J.E. (1996) Genetic requirements for the single-strand annealing pathway of double-strand break repair in *Saccharomyces cerevisiae*. *Genetics*, **142**, 693–704.

26. Shiraishi,K., Hanada,K., Iwakura,Y. and Ikeda,H. (2002) Roles of RecJ, RecO, and RecR in RecET-mediated illegitimate recombination in *Escherichia coli*. *J. Bacteriol.*, **184**, 4715–4721.

27. Kolodner,R., Fishel,R.A. and Howard,M. (1985) Genetic recombination of bacterial plasmid DNA: effect of RecF pathway mutations on plasmid recombination in *Escherichia coli*. *J. Bacteriol.*, **163**, 1060–1066.

28. Sugiyama,T., Kantake,N., Wu,Y. and Kowalczykowski,S.C. (2006) Rad52-mediated DNA annealing after Rad51-mediated DNA strand exchange promotes second ssDNA capture. *EMBO J.*, **25**, 5539–5548.

29. Hobbs,M.D., Sakai,A. and Cox,M.M. (2007) SSB protein limits RecOR binding onto single-stranded DNA. *J. Biol. Chem.*, **282**, 11058–11067.

30. Unciuleac,M.C. and Shuman,S. (2010) Double strand break unwinding and resection by the mycobacterial helicase-nuclease AdnAB in the presence of single strand DNA-binding protein (SSB). *J. Biol. Chem.*, **285**, 34319–34329.

31. Rocha,E.P., Cornet,E. and Michel,B. (2005) Comparative and evolutionary analysis of the bacterial homologous recombination systems. *PLoS Genet.*, **1**, e15.

32. Mizrahi,V. and Andersen,S.J. (1998) DNA repair in *Mycobacterium tuberculosis* What have we learnt from the genome sequence? *Mol. Microbiol.*, **29**, 1331–1339.

33. Marsin,S., Mathieu,A., Kortulewski,T., Guerois,R. and Radicella,J.P. (2008) Unveiling novel RecO distant orthologues involved in homologous recombination. *PLoS Genet.*, **4**, e1000146.

34. Makharashvili,N., Koroleva,O., Bera,S., Grandgenett,D.P. and Korolev,S. (2004) A novel structure of DNA repair protein RecO from *Deinococcus radiodurans*. *Structure*, **12**, 1881–1889.

35. Shereda,R.D., Kozlov,A.G., Lohman,T.M., Cox,M.M. and Keck,J.L. (2008) SSB as an organizer/mobilizer of genome maintenance complexes. *Crit. Rev. Biochem. Mol. Biol.*, **43**, 289–318.

36. Curth,U., Genschel,J., Urbanke,C. and Greipel,J. (1996) *In vitro* and *in vivo* function of the C-terminus of *Escherichia coli* single-stranded DNA binding protein. *Nucleic Acids Res.*, **24**, 2706–2711.

37. Reddy,M.S., Guhan,N. and Muniyappa,K. (2001) Characterization of single-stranded DNA-binding proteins from Mycobacteria. The carboxyl-terminal of domain of SSB is essential for stable association with its cognate RecA protein. *J. Biol. Chem.*, **276**, 45959–45968.

38. Costes,A., Lecointe,F., McGovern,S., Quevillon-Cheruel,S. and Polard,P. (2010) The C-terminal domain of the bacterial SSB protein acts as a DNA maintenance hub at active chromosome replication forks. *PLoS Genet.*, **6**, e1001238.

39. Courcelle,J. and Hanawalt,P.C. (1999) RecQ and RecJ process blocked replication forks prior to the resumption of replication in UV-irradiated *Escherichia coli*. *Mol. Gen. Genet.*, **262**, 543–551.

40. Yadav,T., Carrasco,B., Myers,A.R., George,N.P., Keck,J.L. and Alonso,J.C. (2012) Genetic recombination in *Bacillus subtilis*: a division of labor between two single-strand DNA-binding proteins. *Nucleic Acids Res.*, **40**, 5546–5559.

41. Manfredi,C., Suzuki,Y., Yadav,T., Takeyasu,K. and Alonso,J.C. (2010) RecO-mediated DNA homology search and annealing is facilitated by SsbA. *Nucleic Acids Res.*, **38**, 6920–6929.

42. Manfredi,C., Carrasco,B., Ayora,S. and Alonso,J.C. (2008) *Bacillus subtilis* RecO nucleates RecA onto SsbA-coated single-stranded DNA. *J. Biol. Chem.*, **283**, 24837–24847.